

# UC Santa Barbara

## UC Santa Barbara Previously Published Works

### Title

Switching the aptamer attachment geometry can dramatically alter the signalling and performance of electrochemical aptamer-based sensors

### Permalink

<https://escholarship.org/uc/item/8ds525jk>

### Journal

Chemical Communications, 57(88)

### ISSN

1359-7345

### Authors

Chamorro-Garcia, Alejandro  
Ortega, Gabriel  
Mariottini, Davide  
[et al.](#)

### Publication Date

2021-11-04

### DOI

10.1039/d1cc04557a

Peer reviewed



Published in final edited form as:

*Chem Commun (Camb)*. ; 57(88): 11693–11696. doi:10.1039/d1cc04557a.

## Switching the aptamer attachment geometry can dramatically alter the signalling and performance of electrochemical aptamer-based sensors

Alejandro Chamorro-Garcia<sup>a,b</sup>, Gabriel Ortega<sup>a,c</sup>, Davide Mariottini<sup>b</sup>, Joshua Green<sup>d</sup>,  
Francesco Ricci<sup>b</sup>, Kevin W. Plaxco<sup>\*,a,d</sup>

<sup>a</sup>Center for Bioengineering, University of California Santa Barbara, Santa Barbara, CA 93106, USA.

<sup>b</sup>Dipartimento di Scienze e Tecnologie Chimiche, University of Rome, Tor Vergata, Via della Ricerca Scientifica, 00133 Rome, Italy.

<sup>c</sup>Precision Medicine and Metabolism Laboratory, CIC bioGUNE, Basque Research and Technology Alliance, Parque Tecnológico de Bizkaia, Derio, Spain.

<sup>d</sup>Department of Chemistry and Biochemistry University of California Santa Barbara (UCSB), Santa Barbara, CA 93106, USA.

### Abstract

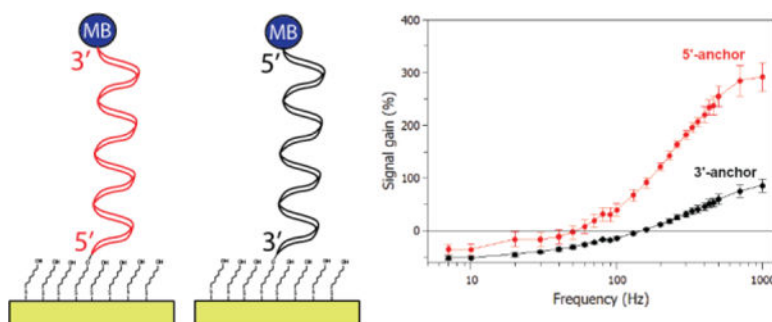
Electrochemical Aptamer-Based (EAB) sensors, composed of an electrode bound DNA aptamer with a redox reporter on the distal end, offer the promise of high-frequency, real-time molecular measurements in complex sample matrices and even in vivo. Here we assess the extent to which switching the aptamer terminus that is electrode bound and the one redox reporter modified affects the performance of these sensors. Using sensors against doxorubicin, cocaine, and vancomycin as our test beds, we find that both signal gain (the relative signal change seen in the presence of saturating target) and the frequency dependence of gain depend strongly on the attachment orientation, suggesting that this easily investigated variable is a worthwhile parameter to optimize in the design of new EAB sensors.

### Graphical Abstract

\*Corresponding author: Kpw@chem.ucsb.edu.

Electronic Supplementary Information (ESI) available: [details of any supplementary information available should be included here].  
See DOI: 10.1039/x0xx00000x

The authors declare the following competing financial interest(s): K.W.P. discloses service on the scientific advisory boards of Diagnostic Biochips Inc. and Nutromics, both of which are developing applications related to this work.



## Text for TOC

Switching which termini the redox reporter and surface-anchoring thiol are on in electrochemical aptamer-based sensors significantly alters their performance.

Because they are reagentless, single step, and able to work directly in highly complex sample matrices, electrochemical aptamer-based (EAB) sensors<sup>1</sup> support the convenient, high-frequency measurement of specific molecular targets both *ex vivo* in unprocessed clinical samples<sup>2</sup> and *in situ* in the living body<sup>3</sup>. Consisting of a redox-reporter-modified aptamer attached to an interrogating electrode surface, EAB sensors produce a signal when binding induces a conformational change in their target-recognizing aptamer. This in turn alters the electron transfer kinetics of the redox reporter, most often methylene blue (MB), which can be monitored electrochemically<sup>4</sup>. Given that this signalling mechanism is independent of the chemical or enzymatic reactivity of the sensor's target, EAB sensors are also generalizable<sup>5</sup>, and can be adapted to new targets via the simple expedient of switching out their recognition aptamer. Consistent with this, EAB sensors have been reported for detection of a wide range of targets, including many proteins<sup>6</sup>, inorganic ions<sup>7</sup>, and small molecules<sup>8</sup>. Finally, due to their conformation-linked signalling, EAB sensors are highly selective and thus, as noted above, even support seconds-resolved, real-time molecular measurements *in situ* in the veins of living animals<sup>3,9</sup>.

A number of design and “interrogation” (electrochemical) parameters have been described to date that affect the performance of EAB sensors<sup>10</sup>. For example, because EAB signalling is driven by binding-induced changes in electron transfer rate, their signal gain (the relative signal change at saturating target -see equation 1 in SI) under square wave voltammetry (SWV) interrogation depends sensitively on the amplitude and frequency of the potential pulse employed<sup>11</sup>. We thus routinely tune both to achieve optimal sensor performance. Gain and, sometimes, affinity are likewise functions of the density with which the target-recognizing aptamer is packed onto its surface and thus we tune this parameter, too, in order to achieve optimal sensor performance<sup>12</sup>. Finally, to support either calibration free *in vitro* performance or drift-free *in vivo* performance we employ approaches that are reliant on the frequency-dependence of signal-gain, with this dependence also being a property that can also be optimized<sup>13</sup>.

In addition to the above-described parameters, recent studies have also shown that the placement of the redox tag in an EAB sensor can significantly alter sensor performance<sup>14</sup>. In

one study, for example, placement of the redox reporter at an internal position on the chain (i.e., not, as has most often been employed, at the distal terminus) was shown to decrease the gain of a sensor<sup>15</sup> for the detection of tumour necrosis factor alpha (TNF- $\alpha$ ) by a factor of 2. Conversely, internal placement of the reporter in the aptamer sequence increased the gain of an insulin-detecting sensor<sup>16</sup> by a factor of 1.5. It is thus clear that redox-reporter placement can alter EAB sensor performance, albeit with the magnitude of any effects likely varying depending on the aptamer's structure and the details of the reporter's placement. Building on these observations, here we explored the extent to which switching which end of the aptamer is attached to the electrode and which is modified with the reporter alters the magnitude and frequency dependence of a sensor's gain. To do so we compared the performance of pairs of sensors in which the thiol group for anchoring the aptamer to the electrode is placed at the 5' terminus and the redox reporter at the 3' terminus with those in which this had been reversed (Fig. 1).

As representative examples to explore the importance of this design parameter we have employed EAB sensors directed against the chemotherapeutic doxorubicin, the drug of abuse cocaine, and antibiotic vancomycin, all of which have previously been described using the commonly employed 5'-anchor (and thus 3' methylene blue) orientation<sup>17</sup>. Indeed, using this 5' anchor orientation, two of these sensors have been shown to support continuous, real-time measurements in situ in the living body<sup>18</sup>. Here, we explore the signal gain and affinity of these sensors as a function of the attachment orientation of their recognition aptamers and of the square-wave frequency employed in their interrogation. Please refer to supporting information for materials and methods and detailed description of the experimental procedures followed. Of note, the gain of EAB sensors is so strongly dependent on that latter parameter<sup>11</sup> that, at some frequencies, they exhibit signal-on behaviour (binding increases the signalling current), whereas at others they are signal-off. This simultaneous signal-on and signal-off behaviour serves as the basis for the most commonly employed drift correction algorithm used to ensure good EAB signal stability in vivo, and thus both behaviours are of importance.

The signalling characteristics of the doxorubicin-detecting sensor change quite significantly upon switching the aptamer's orientation. To see this, we characterized the gain of 3' and 5'-anchored sensors as a function of square wave frequency (Fig. 2A), finding that, while the highest signal-on gain we observe for the 5'-anchor orientation is  $280\pm 30\%$  (unless otherwise noted, the confidence intervals here and elsewhere reflect the standard deviation of 4 replicates from independently fabricated sensors), at 700 Hz, the highest signal-on gain we obtained for the 3'-anchor orientation is only  $85\pm 13\%$  (at 1,000 Hz). The highest magnitude signal-off gain we observed for the two constructs likewise differs, but to a lesser extent, being  $-35\pm 10\%$  for the 5'-anchor orientation (at 5 Hz) and  $-51\pm 3\%$  for the 3'-anchor orientation (at 10 Hz).

To ascertain whether the orientation effects on gain observed for the doxorubicin-binding aptamer hold for other aptamers, we next investigated sensors for the detection of either the drug-of-abuse cocaine (Fig. 2B) or the antibiotic vancomycin (Fig. 2C). Once again, we find that the attachment orientation affects signal gain of both. Specifically, while we observe  $820\pm 80\%$  gain for the 5'-anchor orientation (at 900 Hz) of the cocaine-binding

aptamer, the largest magnitude signal-on gain we observe for its 3'-anchor orientation is only  $169\pm 33\%$  (at 430 Hz). For this sensor, neither orientation produced a signal-off response at any of the frequencies we investigated. Likewise, the vancomycin-detecting sensor reaches  $61\pm 4\%$  signal-on gain (at 60 Hz) in its 5'-anchor orientation, but only  $15\pm 5\%$  (at 50 Hz) in its 3'-anchor orientation, with signal-off gains of  $-38\pm 2\%$  (at 5 Hz) for the 5'-anchor orientation and  $-20\pm 1\%$  (at 5 Hz) for the 3'-anchor orientation. Thus, for all three of the sensors we have explored here, we observe significantly better signal-on gain for the 5'-anchor orientation.

The generally strong frequency dependence of EAB signal gain has been used to perform drift correction for in vivo applications<sup>3</sup>, and for producing calibration-free sensors<sup>19</sup>. This point is sufficiently important that, for those rare EAB sensors for which the gain is only weakly frequency dependent, we have developed new approaches to increasing the frequency dependence of EAB gain to ensure their good in vivo performance<sup>20</sup>. Given this, we note that, for the three sensors we have investigated here, the frequency dependence of their gain is, like their gain itself, also greater for their 5' anchor orientations (Fig. 3). In contrast to the effects of attachment geometry on signal gain, we do not a priori expect the binding properties of the sensor (e.g., the mid-point of its binding response curve) to vary with the attachment geometry, as the structure of the aptamer's binding site should not depend on which of its ends is attached to the surface. Consistent with this, we measured their binding curves (Fig. 4) and found that the affinity of each sensor remains effectively unchanged upon switching the anchoring orientation. This consistency suggests that each aptamer's binding site is unaffected by this change, suggesting in turn that specificity is likely retained.

All three of the sensors explored here exhibit greater signal-on signal gain and stronger frequency-dependent gain when their aptamers are anchored via their 5' termini. Consistent with this, previous studies employing electrode-bound, linear DNA strands to detect DNA hybridization likewise report greater gain for the 5' anchor orientation<sup>21</sup>. Given this, we are tempted to speculate regarding the possible mechanistic origins of such an effect. Specifically, it has previously been shown that short, double-stranded DNAs attached to a surface using a 5' linkage adopt a more vertical orientation (relative to the surface) than those anchored via a 3' linkage, leading to more rapid electron transfer from a reporter on the distal end of the latter<sup>22</sup>. This presumably arises due to subtle changes in the specific geometry of linkages to 3' versus 5' hydroxyl groups which, of course, are not equivalent. As all three of the aptamers we have explored here are thought to bring their two termini together in their bound, folded states, the portion of them closest to the electrode is likely also a double helix and thus likely also subject to this attachment-site orientation effect. This speculation aside, however, it is quite possible that, were we to characterize additional aptamers, we would find some that behave in the inverse manner, with the 3' anchor orientation exhibiting higher signal-on gain and stronger frequency dependence. Fortunately, checking this empirically is simple and convenient.

Optimization of many of the parameters that define the fabrication and interrogation of EAB sensors have seen extensive study. The orientation with which the aptamer is anchored to the sensor surface, however, has not. Here we describe the effects and consequences of

switching the attachment orientation using 3 well-established EAB sensors. Doing this we find that, while affinity remains unchanged for all three sensors, we observe significant differences in both their signal gain and its frequency dependence. In light of these observations, our “take-home message” is that: (1) attachment orientation can alter sensor performance and (2) is a relatively easy parameter to investigate, suggesting that it should be explored in the optimization of new EAB sensors.

## Supplementary Material

Refer to Web version on PubMed Central for supplementary material.

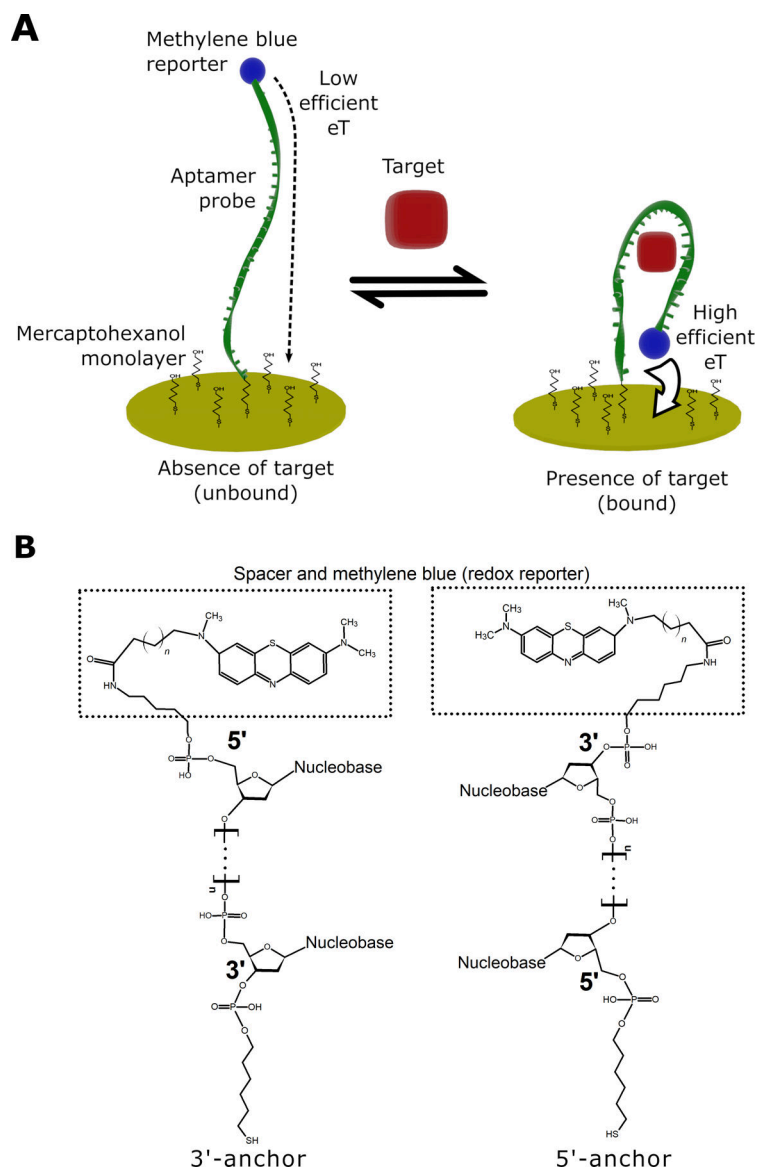
## Acknowledgments

This work was supported by the NIH (R01AI145206). A.C. is a Marie Curie out going fellow Individual Fellowship Global Fellowship (IF-GF) (Proposal 799332 SmartBioSense under call H2020-MSCA-IF-2017).

## References

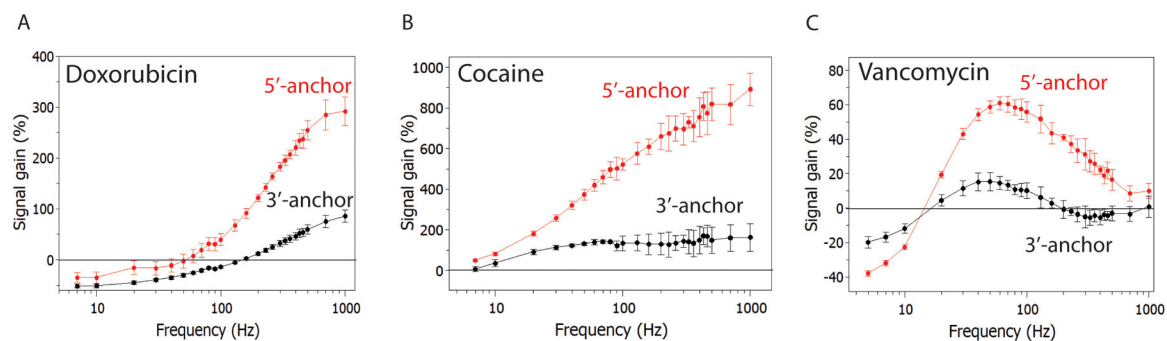
1. Fan C, Plaxco KW, Heeger AJ, Proc. Natl. Acad. Sci. U. S. A 2003, 100, 9134–9137; Y. Xiao, A.A. Lubin, A.J. Heeger, and K.W. Plaxco, Angew. Chem., 2005, 44, 5456–5459; Y. Xiao, R. Lai and K.W. Plaxco, Nat. Protoc., 2007, 2, 2875–2880; L.R. Schoukroun-Barnes, Florika C. Macazo, B. Gutierrez, J. Lottermoser, J. Liu, and R.J. White, Annual Review of Anal. Chem., 2016, 9:1, 163–181. [PubMed: 12867594]
2. Swenson JS, Xiao Y, Ferguson BS, Lai RY, Heeger AJ, Plaxco KW and Soh TJ, J. Am. Chem. Soc, 2009, 131, 4262–4266; R. J. White, H. M. Kallewaard, W. Hsieh, A.S. Patterson, J.B. Kasehagen, K.J. Cash, T. Uzawa, H. T. Soh, and K.W. Plaxco, Anal. Chem., 2012, 84, 1098–1103; A. Vallée-Bélisle, F. Ricci, T. Uzawa, F. Xia and K.W. Plaxco, J. Am. Chem. Soc., 2012, 134, 15197–15200; A. Idili, C. Parolo, G. Ortega and K.W. Plaxco, ACS Sensors, 2019, 4, 3227–3233; [PubMed: 19271708]
3. Arroyo-Currás N, Somerson J, Vieira P, Ploense K, Kippin T and Plaxco KW, Proc. Natl. Acad. Sci, 2017, 114, 645–650; N. Arroyo-Curras, P. Dauphin-Ducharme, G. Ortega, K. Ploense, T. Kippin, and K.W. Plaxco, ACS Sensors, 2018, 3, 360–366; A. Idili, N. Arroyo-Currás, K. L. Ploense, A. T. Csordas, M. Kuwahara, T. E. Kippin and K. W. Plaxco, Chem. Sci., 2019, 10, 8164–8170; [PubMed: 28069939]
4. Plaxco KW, Soh HT, Trends in Biotechnol, 2011, 29, 1–5.
5. Lubin AA and Plaxco KW, Accounts of Chem. Res, 2010, 43, 496–505; L.R. Schoukroun-Barnes, C. F. Macazo, B. Gutierrez, J. Lottermoser, J. Liu and R. J. White, Annu. Rev. Anal. Chem., 2016, 9:1, 163–181.
6. Xiao Y, Lubin AA, Heeger AJ and Plaxco KW. Angew. Chem, 2005, 44, 5456–5459; Y. Xiao, B. D. Piorek, K. W. Plaxco and A. J. Heeger, J. Am. Chem. Soc., 2005, 127, 17990–17991. [PubMed: 16044476]
7. Wu Y and Lai RY, Biotechnol. J, 2016, 11, 788–796. [PubMed: 26901685]
8. Baker BR, Lai RY, Wood MS, Doctor EH, Heeger AJ and Plaxco KW, J. Am. Chem. Soc, 2006, 128, 3138–3139; A. Rowe, E. Miller and K. W. Plaxco, Anal. Chem., 2010, 82, 7090–7095. [PubMed: 16522082]
9. Dauphin-Ducharme P, Yang K, Arroyo-Currás N, Ploense K, Zhang Y, Gerson J, Kurnik M, Kippin TE, Stojanovic M and Plaxco KW, ACS Sensors, 2019, 4, 2832–2837. [PubMed: 31556293]
10. Aller-Pellitero M, Shaver A and Arroyo-Curras N, J. Electrochem. Soc, 2020, 167, 037529.
11. White RJ and Plaxco KW, Anal. Chem, 2010, 82, 73–76; P. Dauphin-Ducharme and K. W. Plaxco, Anal. Chem., 2016, 88, 11654–11662. [PubMed: 20000457]
12. Ricci F, Lai Y, Heeger AJ, Plaxco KW and Sumner JJ, Langmuir, 2007, 23, 6827–6834; R. J. White, K. W. Plaxco, Langmuir, 2008, 24, 10513–10518; B.E. Fernández de Ávila, H.M. Watkins,

- J.M. Pingarrón, K.W. Plaxco KW, G. Palleschi and F. Ricci, *Anal. Chem.*, 2013, 85, 6593–6597. [PubMed: 17488132]
13. White RJ and Plaxco KW, *Anal. Chem.*, 2010, 82, 73–76; H. Li, P. Dauphin-Ducharme, G. Ortega, and K. W. Plaxco, *J. Am. Chem. Soc.*, 2017, 139, 11207–11213. [PubMed: 20000457]
14. Lubin AA, Stoep Hunt BV, White RJ, and Plaxco KW, *Anal. Chem.*, 2009, 81, 2150–2158; S.M. Silva, S. Hoque, V. R. Gonçalves and J. J. Gooding, *Electroanalysis*, 2018, 30, 1529–1535. [PubMed: 19215066]
15. Mayer MD and Lai RY, *Talanta*, 2018, 189, 585–591. [PubMed: 30086964]
16. Gerasimov JY, Schaefer CS, Yang W, Grout RL and Lai RY, *Biosens. and Bioelectron.*, 42, 2013, 62–68.
17. Arroyo-Currás N, Somerson J, Vieira PA, Ploense KL, Kippin TE and Plaxco KW, *Proc. Natl. Acad. Sci.*, 2017, 114, 645–650; B. R. Baker, R. Y. Lai, M. S. Wood, E. H. Doctor, A. J. Heeger, and K. W. Plaxco, *J. Am. Chem. Soc.*, 2006, 128 (10), 3138–3139; P. Dauphin-Ducharme, K. Yang, N. Arroyo-Currás, K. L. Ploense, Y. Zhang, J. Gerson, M. Kurnik, T. E. Kippin, M N. Stojanovic, and K. W. Plaxco, *ACS Sensors*, 2019, 4, 2832–2837. [PubMed: 28069939]
18. Arroyo-Currás N, Somerson J, Vieira PA, Ploense KL, Kippin TE, Plaxco KW, *Proc. Natl. Acad. Sci.*, 2017, 114, 645–650; P. Dauphin-Ducharme, K. Yang, N. Arroyo-Currás, K. L. Ploense, Y. Zhang, J. Gerson, M. Kurnik, T. E. Kippin, M N. Stojanovic, and K. W. Plaxco, *ACS Sensors*, 2019, 4, 2832–2837. [PubMed: 28069939]
19. Li H, Li S, Dai J, Li C, Zhu M, Li H, Lou X, Xia F and Plaxco Kevin W., *Chem. Sci.*, 2019, 10, 10843–10848. [PubMed: 34040713]
20. Idili A, Arroyo-Currás N, Ploense KL, Csordas AT, Kuwahara M, Kippin TE and Plaxco KW, *Chem. Sci.*, 2019, 10, 8164–8170. [PubMed: 31673321]
21. Farjami E, Campos R and Ferapontova EE. *Langmuir*, 2012, 28, 16218–16226. [PubMed: 23106377]
22. Farjami E, Campos R and Ferapontova EE. *Langmuir*, 2012, 28, 16218–16226; M. Sam, E. M. Boon, J. K. Barton, M. G. Hill and E. M. Spain. *Langmuir*, 2001, 17, 5727–5730. [PubMed: 23106377]

**Figure 1.**

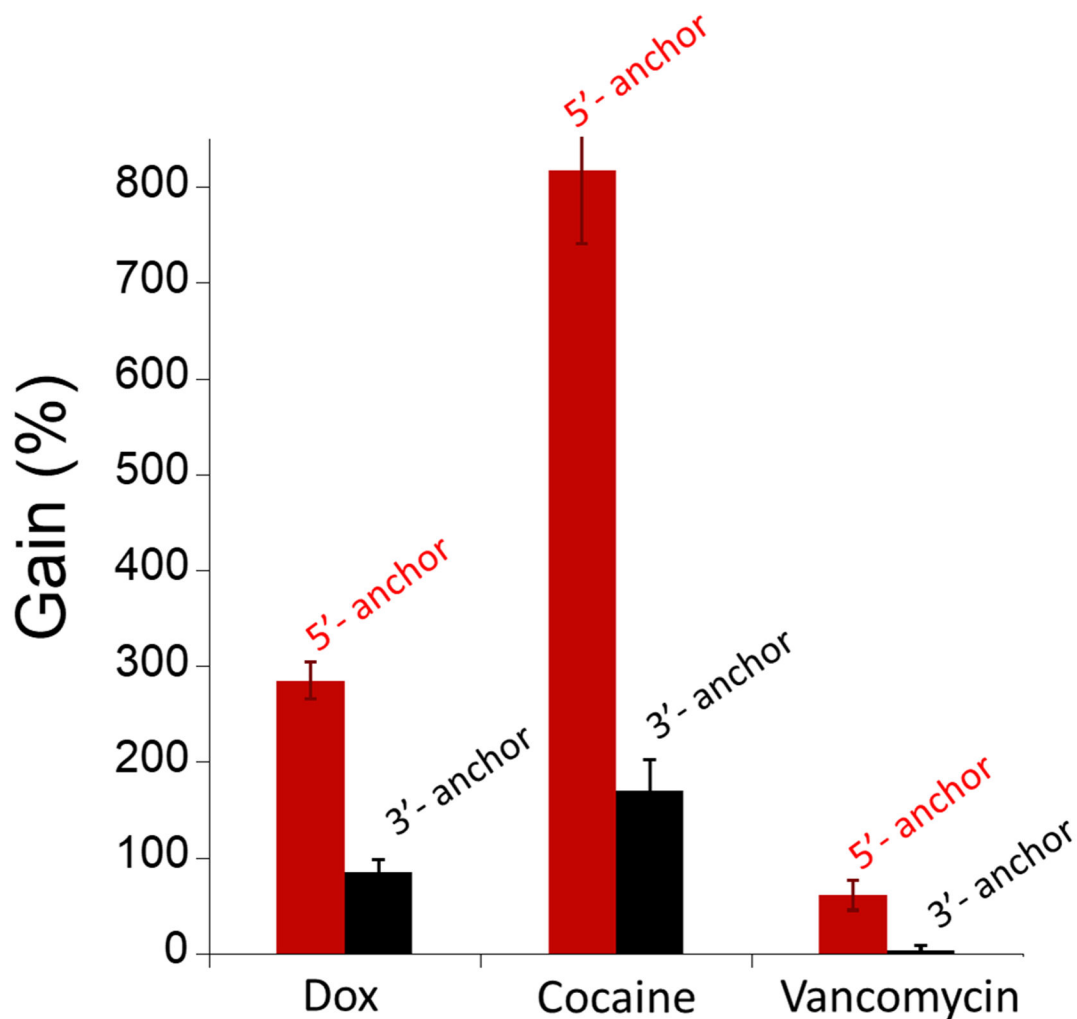
(A) Electrochemical aptamer-based (EAB) sensors are comprised of a target-binding aptamer attached via a thiol on one terminus to an interrogating electrode and modified, typically at the terminus distal to the electrode, with a redox reporter (here methylene blue: MB). Most reports of EAB sensors to date have anchored the aptamer to its interrogating electrode via its 5', with the redox reporter being situated on the 3' end. Here, however, we explore the extent to which the signalling properties of EAB sensors depend on this attachment orientation. (B) That is, we have explored the extent to which gain, the frequency dependence of gain, and target affinity vary when we switch the aptamer's attachment from its 3' end (left panel) to its 5' end (right panel).





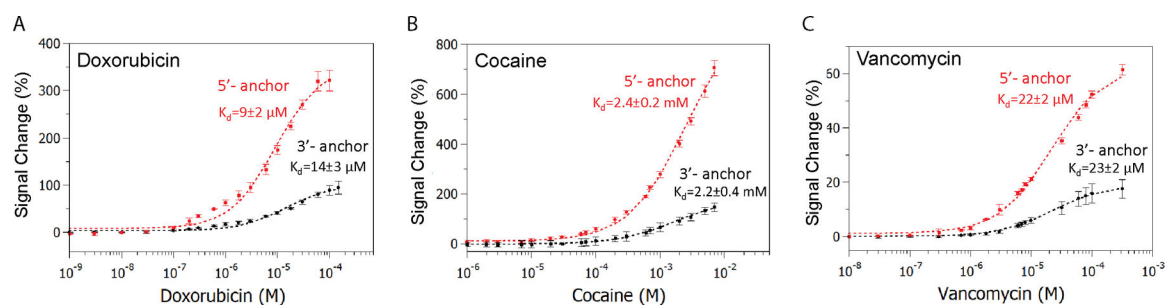
**Figure 2.**

The signaling of electrochemical aptamer-based (EAB) sensors can be a strong function of the attachment orientation of their aptamers, but the extent to which it does varies depending on the aptamer. As shown here, for example, the signal gain of various EAB sensors, which is defined as the relative signal change between the absence of target and saturating target, varies strongly with the attachment orientation. Shown are plots of signal gain as a function of the square-wave interrogation frequency for (A) a doxorubicin-detecting sensor, (B) a cocaine-detecting sensor and (C) a vancomycin-detecting sensor. The error bars here and elsewhere in this paper denote the standard deviation of replicates collected using independently fabricated sensors. As saturating target concentrations, we employed 100  $\mu\text{M}$ , 7 mM or 100  $\mu\text{M}$  in panels A, B, and C, respectively.



**Figure 3:**

The more commonly used 5' anchor orientation achieves notably higher signal-on gain (relative signal change in the presence of saturating target at signal-on square-wave frequencies) for all three of sensor pairs we have investigated here. Shown here, for example, are the largest magnitude signal-on gains we observe for each sensor. Signal-off gain is also a function of the anchor orientation, albeit less so (Fig. S11).

**Figure 4:**

The affinities of the aptamers we have employed are independent of their attachment orientation. Specifically, in the 5'-anchor versus 3'-anchor orientations, we observe binding curve midpoints of  $9 \pm 2 \mu\text{M}$  and  $14 \pm 3 \mu\text{M}$ , respectively, for doxorubicin, (B)  $2.4 \pm 0.2 \text{ mM}$  and  $2.2 \pm 0.4 \text{ mM}$  for cocaine, and (C)  $22 \pm 2 \mu\text{M}$  and  $23 \pm 2 \mu\text{M}$  for vancomycin. Each curve was collected at the frequency at which the highest signal-on gain was observed.